Inferring White Matter Geometry from Diffusion Tensor MRI: Application to Connectivity Mapping

Christophe Lenglet, Rachid Deriche, and Olivier Faugeras

Odyssée Lab, INRIA Sophia-Antipolis, France
{clenglet,der,faugeras}@sophia.inria.fr

Abstract. We introduce a novel approach to the cerebral white matter connectivity mapping from diffusion tensor MRI. DT-MRI is the unique non-invasive technique capable of probing and quantifying the anisotropic diffusion of water molecules in biological tissues. We address the problem of consistent neural fibers reconstruction in areas of complex diffusion profiles with potentially multiple fibers orientations. Our method relies on a global modelization of the acquired MRI volume as a Riemannian manifold M and proceeds in 4 majors steps: First, we establish the link between Brownian motion and diffusion MRI by using the Laplace-Beltrami operator on M. We then expose how the sole knowledge of the diffusion properties of water molecules on M is sufficient to infer its geometry. There exists a direct mapping between the diffusion tensor and the metric of M. Next, having access to that metric, we propose a novel level set formulation scheme to approximate the distance function related to a radial Brownian motion on M. Finally, a rigorous numerical scheme using the exponential map is derived to estimate the geodesics of M, seen as the diffusion paths of water molecules. Numerical experimentations conducted on synthetic and real diffusion MRI datasets illustrate the potentialities of this global approach.

1 Introduction

Diffusion imaging is a magnetic resonance imaging technique introduced in the mid 1980s [1], [2] which provides a very sensitive probe of biological tissues architecture. Although this method suffered, in its very first years, from severe technical constraints such as acquisition time or motion sensitivity, it is now taking an increasingly important place with new acquisition modalities such as ultrafast echo-planar methods. In order to understand the neural fibers bundle architecture, anatomists used to perform cerebral dissection, strychnine or chemical markers neuronography [3]. As of today, diffusion MRI is the unique non-invasive technique capable of probing and quantifying the anisotropic diffusion of water molecules in tissues like brain or muscles. As we will see in the following, the diffusion phenomenon is a macroscopic physical process resulting from the permanent Brownian motion of molecules and shows how molecules tend to move from low to high concentration areas over distances of about 10 to 15 μm during

T. Pajdla and J. Matas (Eds.): ECCV 2004, LNCS 3024, pp. 127–140, 2004.

typical times of 50 to 100 ms. The key concept that is of primary importance for diffusion imaging is that diffusion in biological tissues reflects their structure and their architecture at a microscopic scale. For instance, Brownian motion is highly influenced in tissues such as cerebral white matter or the *annulus fibrosus* of inter-vertebral discs. Measuring, at each voxel, that very same motion along a number of sampling directions (at least 6, up to several hundreds) provides an exquisite insight into the local orientation of fibers and is known as diffusion-weighted imaging. In 1994, Basser et al. [4] proposed the model, now widely used, of the diffusion tensor featuring an analytic means to precisely describe the three-dimensional nature of anisotropy in tissues.

Numerous works have already addressed the problem of the estimation and regularization of these tensor fields. References can be found in [5], [6], [7], [8], [9]. Motivated by the potentially dramatic improvements that knowledge of anatomical connectivity would bring into the understanding of functional coupling between cortical regions [10], the study of neurodegenerative diseases, neurosurgery planning or tumor growth quantification, various methods have been proposed to tackle the issue of cerebral connectivity mapping. Local approaches based on line propagation techniques [11], [12] provide fast algorithms and have been augmented to incorporate some natural constraints such as regularity, stochastic behavior and even local non-Gaussianity ([13], [14], [15], [16], [17], [18], [19], [20]). All these efforts aim to overcome the intrinsic ambiguity of the diffusion tensor related to white matter partial volume effects. Bearing in mind this limitation, they enable us to generate relatively accurate models of the human brain macroscopic three-dimensional architectures. The tensor indeed encapsulates the averaged diffusion properties of water molecules inside a voxel whose typical extents vary from 1 to 3 mm. At this resolution, the contribution to the measured anisotropy of a voxel is very likely to come from different fibers bundles presenting different orientations. This voxel-wise homogeneous Gaussian model thus limits our capacity to resolve multiple fibers orientations since local tractography becomes unstable when crossing artificially isotropic regions characterized by a planar or spherical diffusion profile [8]. On the other side, new diffusion imaging methods have been recently introduced in an attempt to better describe the complexity of water motion but at the cost of increased acquisition times. This is a case of high angular diffusion weighted imaging [21], [22] where the variance of the signal could give important information on the multimodal aspect of diffusion. Diffusion Spectrum Imaging [23], [24] provides, at each voxel, an estimation of the probability density function of water molecules and has been shown to be a particularly accurate means to access the whole complexity of the diffusion process in biological tissues. In favor of these promising modalities, parallel MRI [25] will reduce the acquisition time in a near future and thus permit high resolution imaging.

More global algorithms such as [26] have been proposed to better handle the situations of false planar or spherical tensors (with fibers crossings) and to propose some sort of likelihood of connection. In [27], the authors make use of the major eigenvector field and in [28] the full diffusion tensor provides the metric of a Riemannian manifold but this was not exploited to propose intrinsic schemes.

We derive a novel approach to white matter analysis, through the use of stochastic processes and differential geometry which yield physically motivated distance maps in the brain, seen as a 3-manifold and thus the ability to compute intrinsic geodesics in the white matter. Our goal is to recast the challenging task of connectivity mapping into the natural framework of Riemannian differential geometry. Section 2 starts from the very definition of Brownian motion and show its link to the diffusion MRI signal for linear spaces in terms of its probability density function. Generalization to manifolds involves the introduction of the infinitesimal generator of the Brownian motion. We then solve, in Section 3, the problem of computing the intrinsic distance function from a starting point x_0 in the white matter understood as a manifold. The key idea is that the geometry of the manifold M has a deep impact on the behavior of Brownian motion. We claim that the diffusion tensor can be used to infer geodesic paths on M that coincide with neural tracts since its inverse defines the metric of M. Practically, this means that, being given any subset of voxels in the white matter, we will be able to compute paths most likely followed by water molecules to reach x_0. As opposed to many methods developed to perform tractography, we can now exhibit a bunch of fibers starting from a single point x_0 and reaching potentially large areas of the brain. Efficient numerical implementation is non-trivial and described in Section 4. Results, advantages and drawbacks of the method are presented and discussed in Section 5. We conclude and present potential extensions in Section 6.

2 From Molecular Diffusion to Anatomical Connectivity

2.1 The Diffusion MRI Signal

Diffusion MRI provides the only non-invasive means to characterize molecular displacements, hence its success in physics and chemistry. To measure diffusion in several directions, the Stejskal-Tanner imaging sequence is widely used. It basically relies on two strong gradient pulses positioned before and after the refocusing 180 degrees pulse of a classical spin echo sequence to control the diffusion weighting. For each slice, at least 6 independent gradient directions and 1 unweighted image are acquired to be able to estimate the diffusion tensor $\mathbf{D}$ and probe potential changes of location of water molecules due to Brownian motion. By performing one measurement without diffusion weighting S_0 and one (S) with a sensitizing gradient $\mathbf{g}$, the diffusion coefficient D along $\mathbf{g}$ can be estimated through the relation:

$$S = S_0 \exp(-\gamma^2 \delta^2 (\Delta - \delta/3) |\mathbf{g}|^2 D) \tag{1}$$

where δ is the duration of the gradient pulses, Δ the time between two gradient pulses and γ the gyromagnetic ratio of the hydrogen proton.

2.2 Brownian Motion and Anisotropic Molecular Diffusion

We recall the definition of a Brownian motion in Euclidean space, the simplest Markov process whose stochastic behavior is entirely determined by its initial

distribution μ and its transition mechanism. Transitions are described by a probability density function p or an infinitesimal generator $\mathcal{L}$. In linear homogeneous spaces, p is easily derived as the minimal fundamental solution associated with $\mathcal{L}$ (solution of equation 2). On manifolds, constructing this solution is a tough task, but for our problem, we only need to characterize $\mathcal{L}$. Further details can be found in [29]. We denote by $\mathbf{V}^d = \mathcal{C}([0,\infty[\rightarrow \mathbb{R}^d)$ the set of d-dimensional continuous functions and by $\mathcal{B}(\mathbf{V}^d)$ the topological σ-algebra on $\mathbf{V}^d$. Then,

Definition 1. *A d-dimensional continuous process X is a $\mathbf{V}^d$-valued random variable on a probability space $(\Omega, \mathcal{F}, \mathbb{P})$*

By introducing the time $t \in [0,\infty[$ such that $\forall v \in \mathbf{V}^d$, $v(t) \in \mathbb{R}^d$, a time-indexed collection $\{X_t(\omega)\}$, $\forall \omega \in \Omega$ generates a d-dimensional continuous process if X_t is continuous with probability one. A Brownian motion is characterized by:

Definition 2. *With μ a probability on $(\mathbb{R}^d, \mathcal{B}(\mathbb{R}^d))$, $X_{t_0}, X_{t_1} - X_{t_0}, ..., X_{t_m} - X_{t_{m-1}}$ mutually independent with initial distribution specified by μ and Gaussian distribution for subsequent times (t_i are nonnegative and increasing), a process X_t is called a d-dimensional Brownian motion with initial distribution μ.*

X_t describing the position of water molecules, we now would like to understand how the diffusion behavior of these molecules is related to the underlying molecular hydrodynamics. Diffusion tensor, as thermal or electrical conductivity tensors, belongs to the broader class of general effective property tensors and is defined as the proportionality term between an averaged generalized intensity B and an averaged generalized flux F. In our particular case of interest B is the concentration gradient ∇C and F is the mass flux J such that Fick's law holds: $J = -\mathbf{D}\nabla C$. By considering the conservation of mass, the general diffusion equation is readily obtained:

$$\frac{\partial C}{\partial t} = \nabla.(\mathbf{D}\nabla C) = \mathcal{L}C \tag{2}$$

In anisotropic cerebral tissues, water molecules motion varies in direction depending on obstacles such as axonal membranes. The positive definite order-2 tensor $\mathbf{D}$ has been related [30] to the root mean square of the diffusion distance by $\mathbf{D} = \frac{1}{6t}\langle (x-x_0)(x-x_0)^T \rangle$ ($\langle . \rangle$ denotes an ensemble average). This is directly related to the minimal fundamental solution of equation 2 for an unbounded anisotropic homogeneous medium and the regular Laplacian with initial distribution (obeying the same law as concentration) $\lim_{t\rightarrow 0} p(x|x_0,t) = \delta(x-x_0)$:

$$p(x|x_0,t) = \left(\frac{1}{4\pi|\mathbf{D}|t}\right)^{(d/2)} \exp\left(\frac{-(x-x_0)^T\mathbf{D}^{-1}(x-x_0)}{4t}\right)$$

Also known as the propagator, it describes the conditional probability to find a molecule, initially at position x_0, at x after a time interval t. All the above concepts find their counterparts when moving from linear spaces, such as $\mathbb{R}^d$, to Riemannian manifolds. Explicit derivation of p is non-trivial in that case and the Laplace-Beltrami operator, well known in image analysis [31], will be of particular importance to define $\mathcal{L}$.

3 White Matter as a Riemannian Manifold

3.1 Geometry of a Manifold from Diffusion Processes

We now want to characterize the anisotropic diffusion of water molecules in the white matter exclusively in term of an appropriate infinitesimal generator $\mathcal{L}$. Brownian motions are characterized by their Markovian property and the continuity of their trajectories. They have been, so far, generated from their initial distribution μ and their transition density function p, but they are characterized in terms of $\mathcal{L}$-diffusion processes. Without any further detail, we claim that under some technical hypothesis on $\mathcal{L}$ (with its domain of definition $D(\mathcal{L})$) and on the Brownian motion X_t, it is possible to define an $\mathcal{L}$-diffusion process on a Riemannian manifold M from the d-dimensional stochastic process X_t. We refer the interested reader to [29]. We focus, as in [32], on the case of a diffusion process with time-independent infinitesimal generator $\mathcal{L}$, assumed to be smooth and non-degenerate elliptic. We introduce Δ_M the Laplace-Beltrami differential operator such that, for a function f on a Riemannian manifold M, $\Delta_M f = \mathrm{div}(\mathrm{grad} f)$. In local coordinates $x_1, x_2, ..., x_d$, the Riemannian metric writes in the form $ds^2 = g_{ij}dx_i dx_j$ and the Laplace-Beltrami operator becomes

$$\Delta_M f(x) = \frac{1}{\sqrt{G}} \frac{\partial}{\partial x_j} \left(\sqrt{G} g^{ij} \frac{\partial f}{\partial x_i} \right) = g^{ij}(x) \frac{\partial^2 f}{\partial x_i \partial x_j}(x) + b^i(x) \frac{\partial f}{\partial x_i}(x)$$

where G is the determinant of the matrix $\{g_{ij}\}$ and $\{g^{ij}\}$ its inverse. Moreover,

$$b^i = \frac{1}{\sqrt{G}} \frac{\partial(\sqrt{G} g^{ij})}{\partial x_j} = g^{jk} \Gamma^i_{jk}$$

where Γ^i_{jk} are the Christoffel symbols of the metric $\{g_{ij}\}$. Δ_M is second order, strictly elliptic. At that point of our analysis, it turns out that constructing the infinitesimal generator $\mathcal{L}$ of our diffusion process boils down to (see [33]):

Definition 3. *The operator $\mathcal{L}$ is said to be an intrinsic Laplacian generating a Brownian motion on M if $\mathcal{L} = \frac{1}{2}\Delta_M$.*

Thus, for a smooth and non-degenerate elliptic differential operator on M of the form: $\mathcal{L} = \frac{1}{2} d^{ij}(x) \frac{\partial^2}{\partial x_i \partial x_j}$ we have the

Lemma 1. *If $(d_{ij}(x))_{i,j=1...d}$ denotes the inverse matrix of $(d^{ij}(x))_{i,j=1...d}$, then $g = d_{ij}dx_i dx_j$ defines a Riemannian metric g on M.*

Conclusion: In the context of diffusion tensor imaging, this is of great importance for the following since it means that the diffusion tensor **D** estimated at each voxel actually defines, after inversion, the metric of the manifold. We have made the link between the diffusion tensor data and the white matter manifold geometry through the properties of Brownian motion.

3.2 From Radial Processes to Neural Fibers Recovery

We can now measure in the intrinsic space of the white matter. The fundamental idea of what follows consists of the hypothesis that water molecules starting at a given point x_0 on M, under Brownian motion, will potentially reach any point on M through a unique geodesic. The sole knowledge of the metric g will enable us to actually compute those geodesics on the manifold inferred from the Laplace-Beltrami operator. Considering paths of Brownian motion (ie. fibers in the white matter) as the characteristics lines of the differential operator $\mathcal{L}$ we can easily extend the concept of radial process for that type of stochastic motion on a Riemannian manifold M [34]. Let us fix a reference point $x_0 \in M$ and let $r(x) = \phi(x_0, x)$ be the Riemannian distance between x and x_0. Then we define the radial process $r_t = r(X_t)$. The function $r : M \to \mathbb{R}^+$ has a well behaved singularity at the origin. We make the assumption that M is geodesically complete and recall the notion of exponential map which will be crucial for the numerical computation of neural fibers. We denote by c_e the geodesic with initial condition $c_e(0) = x$ and $c'_e(0) = e$ ($e \in T_xM$). We denote by $E \subset TM$ the set of vectors e such that $c_e(1)$ is defined. It is an open subset of the tangent bundle TM containing the null vectors $0_x \in T_xM$.

Definition 4. *The exponential map* $\mathtt{exp} : E \subset TM \to M$ *is defined by* $\mathtt{exp}(e) = c_e(1)$. *We denote by* $\mathtt{exp}_x$ *its restriction to one tangent space* T_xM.

Hence, in particular, for each unit vector $e \in T_{x_0}M$, there is a unique geodesic $c_e : [0, \infty[\to M$ such that $c'_e(x_0) = e$ and the exponential map gives $c_e(t) = \mathtt{exp}_{x_0}(te)$. For small time steps t, the geodesics $c_e[0, t[$ is the unique distance minimizing geodesic between its endpoints. We need one more notion to conclude this section: the cutlocus of x_0,$\mathtt{Cut}_{x0}$, which will help us to characterize the distance function r. It is nothing but the locus of points where the geodesics starting orthonormally from x_0 stop being optimal for the distance. The radial function $r(x) = \phi(x_0, x)$ is smooth on $M/\mathtt{Cut}_{x0}$ and we have $|\mathrm{grad}\phi(x)| = 1$

Conclusion: We have expressed the distance function on M. The objectives of the following section will be to propose accurate algorithms to compute this function ϕ everywhere on M and then to use it to estimate geodesics (Brownian paths) on this manifold (the brain white matter).

4 Intrinsic Distance Function, Geodesics

4.1 A Level Set Formulation for the Intrinsic Distance Function

We are now concerned with the effective computation of the distance function ϕ from a closed, non-empty subset K of the 3-dimensional, smooth, connected and complete Riemannian manifold (M, g). In the remaining, K will actually be restricted to the single point x_0, origin of a Brownian motion. We will nevertheless formulate everything in term of K since considering the distance to a larger subset of M will be of interest for future work. Let us now further discuss

the notion of distance function on a Riemannian manifold. Given two points $x, y \in M$, we consider all the piecewise differentiable curves joining x to y. Since M is connected, by the Hopf-Rinow theorem, such curves do exist and

Definition 5. *The distance $\phi(x, y)$ is defined as the infimum of the lengths of the $\mathcal{C}^1$ curves starting at x and ending at y.*

Corollary 1. *If $x_0 \in M$, the function $r : M \to \mathbb{R}$ given by $r(x) = \phi(x, x_0)$ is continuous on M but in general it is not everywhere differentiable.*

We consider a general Hamilton-Jacobi partial differential equation with Dirichlet boundary conditions

$$\begin{cases} H(x, D\phi(x)) = 0 \text{ in } M \setminus K \\ \phi(x) = \phi_0(x) \qquad \text{when } x \in K \end{cases}$$

where ϕ_0 is a continuous real function on K and the Hamiltonian $H : M \times T^\star M \to \mathbb{R}$ is a continuous real function on the cotangent bundle. We make the assumption that $H(x, .)$ is convex and we set $\phi_0(x) = 0 \; \forall x \in K$.
We denote by $|v|$ the magnitude of a vector v of TM, defined as $\sqrt{g(v, v)}$. In matrix notation, by forming $\mathbf{G} = \{g_{ij}\}$ the metric tensor, this writes $\sqrt{v^T \mathbf{G} v}$. Then, by setting $H(x, p) = |p| - 1$, we will work on the following theorem (for details on viscosity solutions on a Riemannian manifold, we refer to [35])

Theorem 1. *The distance function ϕ is the unique viscosity solution of the Hamilton-Jacobi problem*

$$\begin{cases} |grad\phi| = 1 \; \textit{in } M \setminus K \\ \phi(x) = 0 \quad \textit{when } x \in K \end{cases} \tag{3}$$

in the class of bounded uniformly continuous functions.

This is the well-known eikonal equation on the Riemannian manifold (M, g). The viscosity solution ϕ at $x \in M$ is the minimum time $t \geq 0$ for any curve γ to reach a point $\gamma(t) \in K$ starting at x with the conditions $\gamma(0) = 0$ and $|\frac{d\gamma}{dt}| \leq 1$. ϕ is the value function of the minimum arrival time problem. This will enable us to solve equation 3 as a dynamic problem and thus to take advantage of the great flexibility of Level Set methods. On the basis of [36], [37], [38] and [39], we reformulate equation 3 by considering ϕ as the zero level set of a function ψ and requiring that the evolution of ψ generates ϕ so that

$$\psi(x, t) = 0 \Leftrightarrow t = \phi(x) \tag{4}$$

Osher ([36]) showed by using Theorem 5.2 from [39] that, under the hypothesis that the Hamiltonian H is independent of ϕ, the level set generated by 4 is a viscosity solution of 3 if ψ is the viscosity solution of

$$\begin{cases} \psi_t + F(t, x, D\psi(t, x)) = 0 \quad \forall t > 0 \\ \psi(x, 0) = \psi_0(x) \end{cases} \tag{5}$$

provided that $F > 0$ and does not change sign. This is typically the case for our anisotropic eikonal equation where the anisotropy directly arises from the manifold topology and not from the classical speed function of initial value problems (which equals 1 everywhere here). To find our solution, all we need to do is thus to evolve $\psi(x,t)$ while tracking, for all x, the time $\bar{t}$ when it changes sign. Now we have to solve 5 with

$$F(t,x,D\psi) = H(t,x,D\psi) + 1 = |\text{grad}\psi|$$

We first recall that for any function $f \in \mathbb{F}$, where $\mathbb{F}$ denotes the ring of smooth functions on M, the metric tensor $\mathbf{G}$ and its inverse define isomorphisms between vectors (in TM) and 1-forms (in $T^\star M$). In particular, the gradient operator is defined as $\text{grad}f = \mathbf{G}^{-1}df$ where df denotes the first-order differential of f. It directly follows that

$$|\text{grad}\psi| = \sqrt{g(\text{grad}\psi, \text{grad}\psi)} = \left(g_{ij} \frac{\partial \psi}{\partial x_l} g^{li} \frac{\partial \psi}{\partial x_k} g^{kj} \right)^{1/2} = \left(\frac{\partial \psi}{\partial x_k} \frac{\partial \psi}{\partial x_l} g^{kl} \right)^{1/2}$$

and we now present the numerical schemes used to estimate geodesics as well as the viscosity solution of

$$\psi_t + |\text{grad}\psi| = 0 \tag{6}$$

4.2 Numerical Scheme for the Distance Function

Numerical approximation of the hyperbolic term in 6 is now carefully reviewed on the well-known basis of available schemes for hyperbolic conservative laws. We seek a three-dimensional numerical flux approximating the continuous flux $|\text{grad}\psi|^2$ and that is consistent and monotone so that it satisfies the usual jump and entropy conditions and converges towards the unique viscosity solution of interest. References can be found in [40]. On the basis of the Engquist-Osher flux [37] and the approach by Kimmel-Amir-Bruckstein for level set distance computation on 2D manifolds [41], we propose the following numerical flux for our quadratic Hamiltonian $d\psi^T \mathbf{G}^{-1} d\psi$:

$$|\text{grad}\psi|^2 = \sum_{i=1}^{3} g^{ii} (\max(D^-_{x_i}\psi, 0)^2 + \min(D^+_{x_i}\psi, 0)^2) +$$
$$\sum_{\substack{i,j=1 \\ i \neq j}}^{3} g^{ij} \text{minmod}(D^+_{x_i}\psi, D^-_{x_i}\psi) \text{minmod}(D^+_{x_j}\psi, D^-_{x_j}\psi)$$

where the $D^\pm_{x_i}\psi$ are the forward/backward approximations of the gradient in x_i. Higher order implementation has also been done by using WENO schemes in order to increase the accuracy of the method. They consist of a convex combination of n^{th} (we take $n = 5$) order polynomial approximation of derivatives [42]. A classical narrow band implementation is used to speed up the computations.

4.3 Numerical Scheme for the Geodesics Estimation

We finally derive an intrinsic method for geodesics computation in order to estimate paths of diffusion on M eventually corresponding to neural fibers tracts. Geodesics are indeed the integral curves of the intrinsic distance function and are classically obtained by back-propagating in its gradient directions from a given point x to the source x_0. Our problem of interest consists of starting from a given voxel of the white matter and of computing the optimal pathway in term of the distance ϕ until x_0 is reached. We propose to take into account the geometry of the manifold during this integration step by making use of the exponential map. If the geodesic $c(s)$ is the parameterized path $c(s) = (c_1(s), ..., c_d(s))$ which satisfies the differential equation

$$\frac{d^2 c_i}{ds^2} = -\Gamma^i_{jk}(c, \frac{dc}{ds})\frac{dc_j}{ds}\frac{dc_k}{ds} \tag{7}$$

where Γ^i_{jk} are the Christoffel symbols of the second kind defined as $\Gamma^i_{jk} = \frac{1}{2}g^{il}\left(\partial g_{kl}/\partial x_j + \partial g_{jl}/\partial x_k - \partial g_{jk}/\partial x_l\right)$. Equation 7 allows us to write $\mathtt{exp}$ in local coordinates around a point $x \in M$ as

$$c_i(\mathtt{exp}(X)) = X_i - \frac{1}{2}\Gamma^i_{jk}X_jX_k + \mathcal{O}(|X|^3) \quad \forall i = 1, ..., d$$

where X will be identified with the gradient of the distance function at x and derivatives of the metric are estimated by appropriate finite differences schemes. This leads to a much more consistent integration scheme on M.

5 Evaluation on Synthetic and Real Datasets

We have experimented with line propagation local methods which only produce macroscopically satisfying results. With trilinear interpolation of the tensor field and a 4^{th} order Runge Kutta integration scheme, we used the advection-diffusion method [13] and obtained the results on Figure 1. Our global approach is actually more concerned to resolve local ambiguities due to isotropic tensors. We consider synthetic and real data[1] to quantify the quality of the estimated distance functions with upwind and WENO5 finite differences schemes. Our criterion is the a posteriori evaluated map $|\mathrm{grad}\phi|$ which must be equal to 1 everywhere except at the origin x_0. As shown on Figure 2 [left], synthetic data corresponds to an anisotropic non-homogeneous medium for which the diffusion paths describe three (independently homogeneous) intersecting cylinders oriented along the x, y and z axis. It results perfectly isotropic tensors at the intersection of the three cylinders, surrounded by planar tensors in the area where only two cylinders cross each others. Though simple, it is a typical configuration where local methods become unreliable. x_0 denotes the origin of the distance function whose

[1] The authors would like to thank J.F. Mangin and J.B Poline, CEA-SHFJ/Orsay, France for providing us with the data

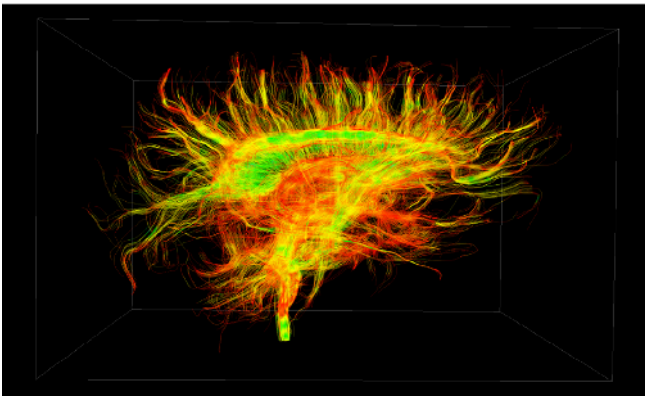

Fig. 1. Neural tracts estimated by the advection-diffusion based propagation method

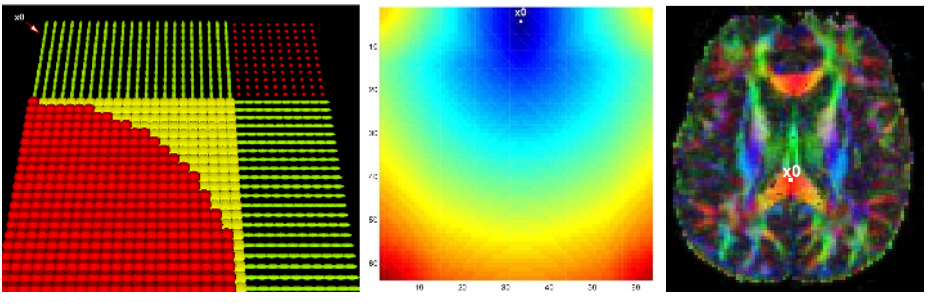

Fig. 2. [left]: Synthetic tensor field (partial), [center]: Associated distance function [right]: Real diffusion tensor MRI (RGB mapping of the major eigenvector)

Table 1. Statistics on $|\text{grad}\phi|$ for synthetic and real diffusion tensor MRI data

DataSet	Scheme	Mean	Std. Dev	Maximum
Synthetic	**Upwind**	0.9854	0.123657	4.50625
Synthetic	**WENO5**	0.977078	0.116855	2.0871
DT-MRI	**Upwind**	0.994332	0.116326	4.80079
DT-MRI	**WENO5**	0.973351	0.110364	3.72567

estimation with the level set scheme proposed in the previous section exhibits very good results in table 1 with a sensible improvement when using WENO5 schemes. The solution of equation 6 along the axis associated to the cylinder containing x_0 is presented on Figure 2 [center]. The recovery of the underlying pathways reaching x_0 by our intrinsic method turns out to be fast in practice and accurate. Figure 3 [left] shows the computed geodesics linking x_0 to anisotropic voxels located at the extremity of a different cylinder. This is basically what happens in the brain white matter when multiple fibers bundles pass through a single voxel. Our global approach seems particularly adequate to disambiguate

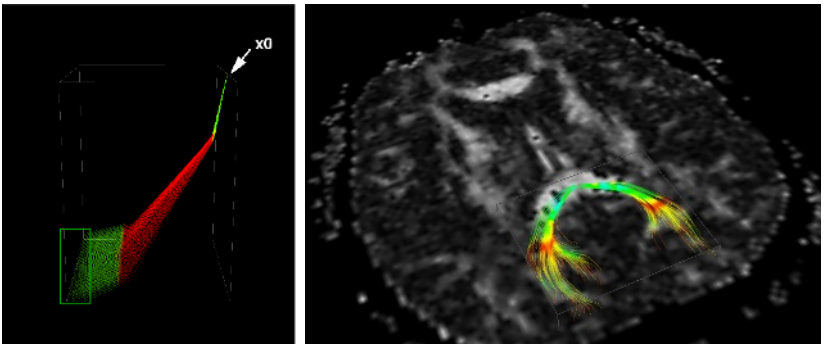

Fig. 3. Inferred geodesics by intrinsic integration - [left]: synthetic [right]: real data

the problem of fibers tracts crossings by minimizing the geodesic distance in the white matter.

Real diffusion data on Figure 2 [right] is used to focus on the posterior part of the corpus callosum. Estimation of the distance function with upwind and WENO5 schemes produces again very good results with evident advantage in term of robustness for WENO implementation. We must notice here that our numerical flux tends to be a bit diffusive, resulting in smooth distance functions. This may be a problem if the original data itself does not have a good contrast since this could yield geodesics with very low curvature. Exponential map based integration produces the result of Figure 3 [right] when starting from the extremities of the major forceps. We have noticed that our method is not influenced by locally spherical or planar tensors since the estimated fibers are not affected by the presence of lower anisotropy regions (in red) that coincide with crossings areas. This global approach thus brings coherence into diffusion tensor data and naturally handles the issues affecting local tractography methods like inconsistent tracking in locally isotropic areas.

6 Conclusion

Diffusion imaging is a truly quantitative method which gives direct insight into the physical properties of tissues through the observation of random molecular motion. However correct interpretation of diffusion data and inference of accurate information is a very challenging project. Our guideline has been to always bear in mind that the true and unique phenomenon that diffusion imaging records is Brownian motion. Taking that stochastic process as our starting point, we have proposed a novel global approach to white matter connectivity mapping. It relies on the fact that probing and measuring a diffusion process on a manifold M provides enough information to infer the geometry of M and compute its geodesics, corresponding to diffusion pathways. Clinical validation is obviously needed but already we can think of extensions of this method: intrinsic geodesics regularization under action of scalar curvature of M, geodesics classification to

recover complete tracts. Estimation of geodesics deviation could be used to detect merging or fanning fiber bundles.

References

1. Bihan, D.L., Breton, E., Lallemand, D., Grenier, P., Cabanis, E., Laval-Jeantet, M.: MR imaging of intravoxel incoherent motions: Application to diffusion and perfusion in neurologic disorders. Radiology (1986) 401–407
2. Merboldt, K., Hanicke, W., Frahm, J.: Self-diffusion nmr imaging using stimulated echoes. J. Magn. Reson. **64** (1985) 479–486
3. Selden, N., Gitelman, D., Salamon-Murayama, N., Parrish, T., Mesulam, M.: Trajectories of cholinergic pathways within the cerebral hemispheres of the human brain. Brain **121** (1998) 2249–2257
4. Basser, P., Mattiello, J., LeBihan, D.: Estimation of the effective self-diffusion tensor from the NMR spin echo. Journal of Magnetic Resonance **B** (1994) 247–254
5. Tschumperlé, D., Deriche, R.: Variational frameworks for DT-MRI estimation, regularization and visualization. In: Proceedings of ICCV. (2003)
6. Chefd'hotel, C., Tschumperlé, D., Deriche, R., Faugeras, O.: Constrained flows on matrix-valued functions : application to diffusion tensor regularization. In: Proceedings of ECCV. (2002)
7. Coulon, O., Alexander, D., Arridge, S.: A regularization scheme for diffusion tensor magnetic resonance images. In: Proceedings of IPMI. (2001)
8. Westin, C., Maier, S., Mamata, H., Nabavi, A., Jolesz, F., Kikinis, R.: Processing and visualization for diffusion tensor MRI. In: Proceedings of Medical Image Analysis. Volume 6. (2002) 93–108
9. Wang, Z., Vemuri, B., Chen, Y., Mareci, T.: Simultaneous smoothing and estimation of the tensor field from diffusion tensor MRI. In: Proceedings of CVPR Volume I., (2003) 461–466
10. Guye, M., Parkera, G.J., Symms, M., Boulby, P., Wheeler-Kingshott, C., Salek-Haddadi, A., Barker, G., Duncana, J.: Combined functional MRI and tractography to demonstrate the connectivity of the human primary motor cortex in vivo. NeuroImage **19** (2003) 1349–1360
11. Mori, S., Crain, B., Chacko, V., Zijl, P.V.: Three-dimensional tracking of axonal projections in the brain by magnetic resonance imaging. Annals of Neurology **45** (1999) 265–269
12. Zhukov, L., Barr, A.: Oriented tensor reconstruction: Tracing neural pathways from diffusion tensor MRI. In: Proceedings of Visualization. (2002) 387–394
13. Lazar, M., Weinstein, D., Tsuruda, J., Hasan, K., Arfanakis, K., Meyerand, M., Badie, B., Rowley, H., V.Haughton, Field, A., Alexander, A.: White matter tractography using diffusion tensor deflection. In: Human Brain Mapping. Volume 18. (2003) 306–321
14. Basser, P., Pajevic, S., Pierpaoli, C., Duda, J., Aldroubi, A.: In vivo fiber tractography using DT-MRI data. Magn. Res. Med. **44** (2000) 625–632
15. Vemuri, B., Chen, Y., Rao, M., McGraw, T., Mareci, T., Wang, Z.: Fiber tract mapping from diffusion tensor MRI. In: Proceedings of VLSM. (2001)
16. Campbell, J., Siddiqi, K., Vemuri, B., Pike, G.: A geometric flow for white matter fibre tract reconstruction. In: Proceedings of ISBI. (2002) 505–508
17. Tuch, D.: Mapping cortical connectivity with diffusion MRI. In: Proceedings of ISBI. (2002) 392–394

18. Hagmann, P., Thiran, J., Jonasson, L., Vandergheynst, P., Clarke, S., Maeder, P., Meuli, R.: DTI mapping of human brain connectivity: Statistical fiber tracking and virtual dissection. NeuroImage **19** (2003) 545–554
19. Bjornemo, M., Brun, A., Kikinis, R., Westin, C.: Regularized stochastic white matter tractography using diffusion tensor MRI. In: Proceedings of MICCAI. (2002) 435–442
20. Parker, G., Alexander, D.: Probabilistic monte carlo based mapping of cerebral connections utilising whole-brain crossing fibre information. In: Proceedings of IPMI. (2003) 684–695
21. Tuch, D., Reese, T., Wiegell, M., Makris, N., Belliveau, J., Wedeen, V.: High angular resolution diffusion imaging reveals intravoxel white matter fiber heterogeneity. Magn. Res. Med. **48** (2002) 577–582
22. Frank, L.: Characterization of anisotropy in high angular resolution diffusion-weighted MRI. Magn. Res. Med **47** (2002) 1083–1099
23. Tuch, D., Wiegell, M., Reese, T., Belliveau, J., Weeden, V.: Measuring cortico-cortical connectivity matrices with diffusion spectrum imaging. In: Int. Soc. Magn. Reson. Med. Volume 9. (2001) 502
24. Lin, C., Weeden, V., Chen, J., Yao, C., Tseng, W.I.: Validation of diffusion spectrum magnetic resonance imaging with manganese-enhanced rat optic tracts and ex vivo phantoms. NeuroImage **19** (2003) 482–495
25. Bammer, R., Auer, M., Keeling, S., Augustin, M., Stables, L., Prokesch, R., Stollberger, R., Moseley, M., Fazekas, F.: Diffusion tensor imaging using single-shot sense-EPI. Magn. Res. Med. **48** (2002) 128–136
26. Mangin, J.F., Poupon, C., Cointepas, Y., Rivière, D., Papadopoulos-Orfanos, D., Clark, C.A., Régis, J., Bihan, D.L.: A framework based on spin glass models for the inference of anatomical connectivity from diffusion-weighted MR data. NMR in Biomedicine **15** (2002) 481–492
27. Parker, G., Wheeler-Kingshott, C., Barker, G.: Estimating distributed anatomical connectivity using fast marching methods and diffusion tensor imaging. Trans. Med. Imaging **21** (2002) 505–512
28. O'Donnell, L., Haker, S., Westin, C.: New approaches to estimation of white matter connectivity in diffusion tensor MRI: Elliptic PDEs and geodesics in a tensor-warped space. In: Proceedings of MICCAI. (2002) 459–466.
29. Ikeda, N., Watanabe, S.: Stochastic Differential Equations and Diffusion Processes. North-Holland Mathematical Library (1989)
30. Einstein, A.: Investigations on the Theory of the Brownian Movement. Dover Pubns (1956)
31. Sochen, N., Deriche, R., Lopez-Perez, L.: The beltrami flow over implicit manifolds. In: Proceedings of ICCV. (2003)
32. de Lara, M.: Geometric and symmetry properties of a nondegenerate diffusion process. An. of Probability **23** (1995) 1557–1604
33. Liao, M.: Symmetry groups of markov processes. Anal. of Prob. **20** (1992) 563–578
34. Hsu, E.: Stochastic Analysis on Manifolds. Volume 38 of Graduate Studies in Mathematics. AMS (2001)
35. Mantegazza, C., Mennucci, A.: Hamilton–jacobi equations and distance functions on Riemannian manifolds. App. Math. and Optim. **47** (2002) 1–25
36. Osher, S.: A level set formulation for the solution of the dirichlet problem for a hamilton-Jacobi equations. SIAM Journal on Mathematical Analysis **24** (1993) 1145–1152
37. Sethian, J.: Level Set Methods. Cambridge University Press (1996)

38. Tsai, Y.H., Giga, Y., Osher, S.: A level set approach for computing discontinuous solutions of Hamilton–Jacobi equations. Math. Comput. **72** (2003) 159–181
39. Chen, Y., Giga, Y., Goto, S.: Uniqueness and existence of viscosity solutions of generalized mean curvature flow equations. Journal on Differential Geometry **33** (1991) 749–786
40. LeVeque, R.: Numerical methods for conservation laws. Birkhäuser, Basel (1992)
41. Kimmel, R., Amir, A., Bruckstein, A.: Finding shortest paths on surfaces using level set propagation. Transactions on Pattern Analysis and Machine Intelligence **17** (1995) 635–640
42. Liu, X., Osher, S., Chan, T.: Weighted essentially non oscillatory schemes. J. Comput. Phys. **115** (1994) 200–212